

## Optical and dielectric dispersion in the Ge/In<sub>2</sub>Se<sub>3</sub>/Ga<sub>2</sub>S<sub>3</sub> interfaces

A. F. Qasrawi<sup>a,b,\*</sup>, O. A. Omareya<sup>a</sup>

<sup>a</sup>*Departments of Physics, Arab American University, Jenin, Palestine*

<sup>b</sup>*Department of Electrical and Electronics Engineering, Istinye University, 34010, Istanbul, Turkey*

In this article, the optical and dielectric performance of the Ge, Ge/In<sub>2</sub>Se<sub>3</sub> and Ge/In<sub>2</sub>Se<sub>3</sub>/Ga<sub>2</sub>S<sub>3</sub> interfaces are reported and discussed. The growth nature of the physically vacuum deposited thin film layers is investigated by means of X-ray diffraction and energy dispersive X-ray spectroscopy. Each 200 nm thick layer exhibited an amorphous type of crystallization with appropriate atomic stoichiometry. Optically, the Ge/In<sub>2</sub>Se<sub>3</sub>/Ga<sub>2</sub>S<sub>3</sub> system is found to exhibit a conduction and a valence band offsets of values of 0.53 and 0.47 eV at the Ge/In<sub>2</sub>Se<sub>3</sub> and of values of 0.30 and 0.70 eV at the In<sub>2</sub>Se<sub>3</sub>/Ga<sub>2</sub>S<sub>3</sub> interfaces, respectively. The values are high enough to actualize quantum confinements in the heterojunction device. The formed double and three layers displayed higher light absorbability than single layers. On the other hand, the dielectric dispersion analysis has shown a wide tunability in the dielectric property in visible light and near IR regions. The dielectric responses at the Ge/In<sub>2</sub>Se<sub>3</sub> and at the Ge/In<sub>2</sub>Se<sub>3</sub>/Ga<sub>2</sub>S<sub>3</sub> interfaces are linear below 2.10 eV and 1.53 eV, respectively. The modeling of the dielectric function revealed the optical conductivity parameters presented by the drift mobility, scattering time, plasmon frequency and free electron density. It was observed that the quantum confinement at the Ge/In<sub>2</sub>Se<sub>3</sub> interfaces improved both of the drift mobility and made the scattering time longer at femtosecond levels. The establishing of the second quantum confinement at the second interface In<sub>2</sub>Se<sub>3</sub>/Ga<sub>2</sub>S<sub>3</sub> raised the drift mobility more and extended the scattering time further. With the estimated plasmon frequencies, the formation of the Ge/In<sub>2</sub>Se<sub>3</sub>/Ga<sub>2</sub>S<sub>3</sub> interface appears to be promising for use in optoelectronic device production especially in photodetection issues.

(Received December 11, 2021; Accepted May 2, 2022)

*Keywords:* Nanosandwich; Dielectric; Plasmon devices; Ge substrate

### 1. Introduction

Heterojunction devices that are fabricated onto germanium substrate are of interest as they show wide range of applications. As for example, Ge/Si field effect tunneling transistors which shows good performance as MOS type device finds switching application were also found suitable for biosensing issues [1]. The Ge/Si heterojunction devices are reported to be ideal for limiting power consumption in MOSFETs. It is regarded as ultra-low power transistors which can offer very steep inverse subthreshold swing slopes to keep the leakage current at low levels [2]. In another work, the heterojunctions made of Ge/Si are found ideal substrates to grow high mobility graphene layers [3]. On the other hand, amorphous InSe which exhibits second-order nonlinear optical properties presented by the strong and photostable second-harmonic generation [4] are also promising for optoelectronic application.

In some of recent works [5, 6], it was shown that, the sandwiching of Ge film between two films of InSe [5] increased the drift mobility values of InSe from 10 cm<sup>2</sup>/Vs to ~42 cm<sup>2</sup>/Vs [5]. We have also considered the design and characterization of the Ge/Ga<sub>2</sub>S<sub>3</sub> interface as remarkable plasmon interface being attractive heterojunction for use as microwave cavities and as wireless terahertz receivers. This system exhibited electron-plasmon coupling frequency in the range of

---

\* Corresponding author: atef.qasrawi@aaup.edu  
<https://doi.org/10.15251/CL.2022.195.319>

1.33-2.30 GHz with drift mobility of charge carriers of  $15.61 \text{ cm}^2/\text{Vs}$  [6]. These two recent works motivated us to bring these three materials (Ge, InSe and  $\text{Ga}_2\text{S}_3$ ) together as stacked heterojunction layers and study their properties as optical and dielectric interfaces. Particularly, here in this work, we will report and discuss the optical properties of the  $\text{Ge}/\text{In}_2\text{Se}_3/\text{Ga}_2\text{S}_3$  interfaces as plasmon heterojunction. The optical energy band gaps, the conduction and valence band offsets as well as the real and imaginary parts of the dielectric functions will be studied and modeled to investigate the necessary optical conduction parameters that dominate the device for visible light communications as optoelectronic receivers.

## 2. Experimental details

The Ge, InSe and  $\text{Ga}_2\text{S}_3$  thin films are prepared from the source materials germanium (99.999%) metal basis,  $\alpha\text{-In}_2\text{Se}_3$  (99.99) crystal lumps and  $\text{Ga}_2\text{S}_3$  (99.99%) powders, respectively. The Ge thin film which was grown onto glass substrates and was monitored by an in situ thickness monitor was of 200 nm thicknesses. The same films are used as substrate to deposit InSe films of thickness of 200 nm. The resulting  $\text{Ge}/\text{In}_2\text{Se}_3$  double layer was coated with a 200 nm  $\text{Ga}_2\text{S}_3$  film. The geometrical design of the three layers are shown in the inset of Fig. 1 (a). The X-ray diffraction technique using Miniflex 600 was used to investigate the crystalline nature of the three layers. The compositional analysis of the films were carried out with the help of energy dispersive X-ray analyzer. The optical transmittance and reflectance spectra at normal incidence were recorded with the help of an Evolution 300-spectrophotometer.

## 3. Results and discussion

In order to reveal information about the crystalline nature of the stacked layers of the  $\text{Ge}/\text{In}_2\text{Se}_3/\text{Ga}_2\text{S}_3$  heterojunction device, the X-ray diffraction (XRD) technique is employed.

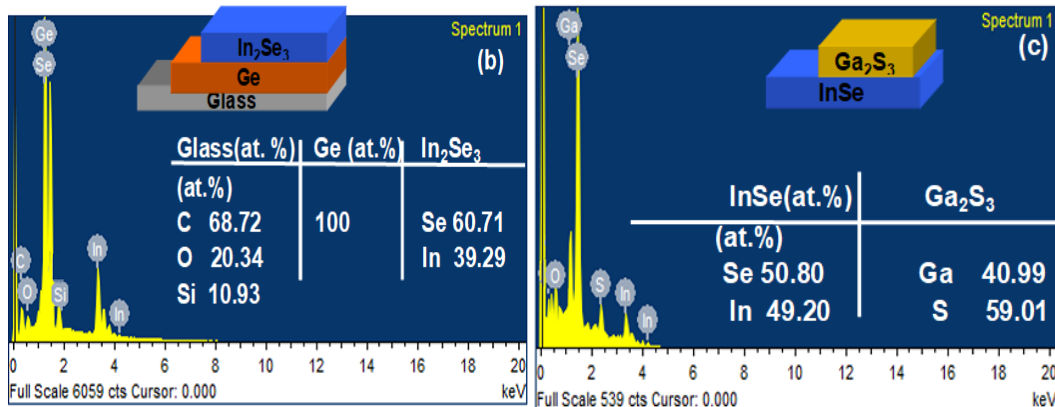
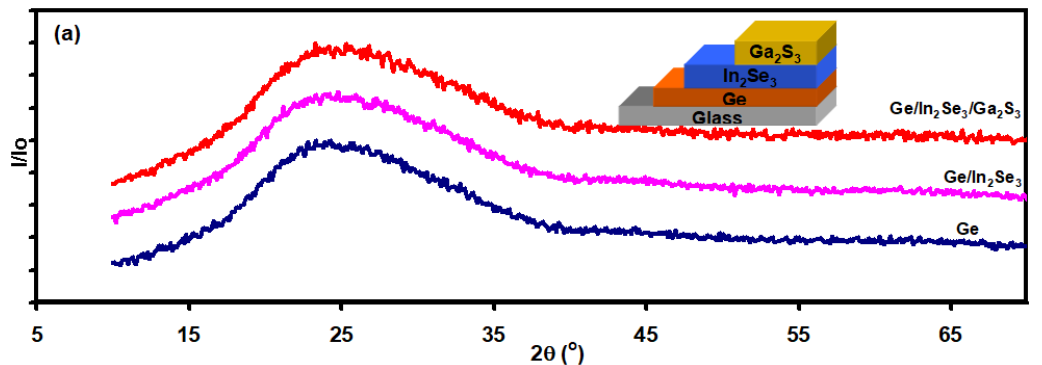


Fig. 1. (a) The X-ray diffraction patterns for the Ge, Ge/In<sub>2</sub>Se<sub>3</sub> and Ge/In<sub>2</sub>Se<sub>3</sub>/Ga<sub>2</sub>S<sub>3</sub> interfaces.

The collected data of the XRD are shown in Fig. 1 (a). As seen from the figure, no sharp peaks can be detected for any of the layers indicating the amorphous nature of crystallization. The lack of the structural information about the nature of the materials composing the heterojunction layers, make prediction of the material formation ambiguous, for this reason the energy dispersion X-ray analysis technique was employed (EDS). The results of the EDS are also displayed in Fig. 1 (b) for the Ge/In<sub>2</sub>Se<sub>3</sub> and in Fig.1 (c) for the In<sub>2</sub>Se<sub>3</sub>/Ga<sub>2</sub>S<sub>3</sub> interfaces. The spectra which were recorded from the top of the Ge/In<sub>2</sub>Se<sub>3</sub> double layer contained the O, C and Si as elements which do exist in the glass substrate, followed by the Ge as pure material and the indium selenide with atomic contents of Se and In of 60.71% and 39.29%, respectively. The preferred stoichiometric composition phase of InSe is In<sub>2</sub>Se<sub>3</sub> when the InSe is grown onto Ge substrate. On the other hand, the data which are illustrated in Fig. 1 (c) suggest that the preferred stoichiometric composition of the gallium sulfide to be Ga<sub>2</sub>S<sub>3</sub> when deposited onto indium monoselenide. The quantitative data that are collected from the EDS technique suggest the physical nature of the growth of the material. The peak of oxygen which appeared in the InSe/Ga<sub>2</sub>S<sub>3</sub> spectra is probably due to the glass substrate as the grown layer of InSe and InSe/Ga<sub>2</sub>S<sub>3</sub> was left to cool for a long period of time in vacuum media and as it was not subjected to air while it was hot.

The optical properties of the three layers are investigated at room temperature in the incident light wavelength range of 300-1100 nm. Fig. 2 (a) show the transmission coefficient spectra ( $T\%$ ) for the Ge, Ge/In<sub>2</sub>Se<sub>3</sub> and Ge/In<sub>2</sub>Se<sub>3</sub>/Ga<sub>2</sub>S<sub>3</sub>, respectively. It is clear from the figure that the transmission coefficient values of Ge which was continuously increasing with increasing wavelength ( $\lambda$ ) tend to remain constant for all  $\lambda > 650 \text{ nm}$  upon deposition of In<sub>2</sub>Se<sub>3</sub> onto Ge. Similarly, the evaporation of the Ga<sub>2</sub>S<sub>3</sub> onto the surface of InSe increased the transmission coefficient. The  $T\%$  values of the Ge/In<sub>2</sub>Se<sub>3</sub> increased from 33% to 59% at 880 nm where the transmission coefficient of the Ge/In<sub>2</sub>Se<sub>3</sub>/Ga<sub>2</sub>S<sub>3</sub> exhibited the absolute maxima. The increase in the transmission coefficient upon participation of Ga<sub>2</sub>S<sub>3</sub> may be assigned to the changes in the band structure of the heterojunction which lead to saturated absorption and nonlinear phase shift [7]. The presence of antireflection surfaces (Ga<sub>2</sub>S<sub>3</sub>) is also believed to be a main reason of the increase in the transmission coefficient values [8]. On the other hand, the reflection coefficient spectra ( $R\%$ ) of the Ge, Ge/In<sub>2</sub>Se<sub>3</sub> and Ge/In<sub>2</sub>Se<sub>3</sub>/Ga<sub>2</sub>S<sub>3</sub> which appears in Fig. 2 (b) display higher reflectivity for Ge than that of Ge/In<sub>2</sub>Se<sub>3</sub> for all  $\lambda < 950 \text{ nm}$ . The Ge/In<sub>2</sub>Se<sub>3</sub> interfaces exhibits an absolute minima at 580 nm. The deposition of the 200 nm thick Ga<sub>2</sub>S<sub>3</sub> onto the surface of Ge/In<sub>2</sub>Se<sub>3</sub> caused the appearance of two resonance peaks at 360 and 610 nm. For all  $\lambda > 670 \text{ nm}$  the  $R\%$  values of Ge/In<sub>2</sub>Se<sub>3</sub>/Ga<sub>2</sub>S<sub>3</sub> are much lower than that of the Ge/In<sub>2</sub>Se<sub>3</sub>. The presence of the absolute minima in the spectra of the Ge/In<sub>2</sub>Se<sub>3</sub> interfaces and the appearance of the two maxima in the reflection coefficient spectra of Ge/In<sub>2</sub>Se<sub>3</sub>/Ga<sub>2</sub>S<sub>3</sub> should be assigned to the interference between the incident light waves with those reflected from the bottom of the film at the glass, Ge and In<sub>2</sub>Se<sub>3</sub> surfaces. The decrease in the values of the reflection coefficient via coating of In<sub>2</sub>Se<sub>3</sub> onto Ge and coating of Ga<sub>2</sub>S<sub>3</sub> onto the surface of In<sub>2</sub>Se<sub>3</sub> should be attributed to the behavior of these layers as antireflection surfaces [8].

Fig. 2 (c) show the absorbance spectra ( $A\% = 100 - T\% - R\%$ ) for the studied interfaces. It is clear from the figure, that the absorbance significantly increased by the coating of Indium selenide onto the surface of Ge. The absorbance spectra for the Ge/In<sub>2</sub>Se<sub>3</sub> and Ge/In<sub>2</sub>Se<sub>3</sub>/Ga<sub>2</sub>S<sub>3</sub> exhibit a sharp decay  $A\%$  values for all  $\lambda < 700 \text{ nm}$ . For larger  $\lambda$  values the decrease in the absorbance percentage with increasing incident light wavelength is smoother than the other region. In addition, the absorbance spectra of the Ge/In<sub>2</sub>Se<sub>3</sub>/Ga<sub>2</sub>S<sub>3</sub> exhibit a peak at 440 nm. The peak refers to a photon energy of 2.82 eV. This value is close to the energy band gap of Ga<sub>2</sub>S<sub>3</sub> [6]. The enhancements in the absorbability of Ge and Ge/In<sub>2</sub>Se<sub>3</sub> are better screened in Fig. 3 (a) which shows the absorption ratio spectra  $R_\lambda = A_x/A_{Ge}$  ( $x$  refer to Ge/In<sub>2</sub>Se<sub>3</sub> or Ge/In<sub>2</sub>Se<sub>3</sub>/Ga<sub>2</sub>S<sub>3</sub>). As the figure shows, the absorption ratio in the Ge/In<sub>2</sub>Se<sub>3</sub> is always greater than one. It exhibits two peaks at 2.62 and 1.65 eV. The absorbability of the Ge/In<sub>2</sub>Se<sub>3</sub> interface reaches  $\sim 1.71$  times in the IR region. The coating of Ga<sub>2</sub>S<sub>3</sub> enhanced the absorption ratio more. The  $R_\lambda$  spectra for the Ge/In<sub>2</sub>Se<sub>3</sub>/Ga<sub>2</sub>S<sub>3</sub> interface reach a maxima of 1.82 at 2.22 eV. The width of the absorption peak at half maximum is 0.91 eV which is narrower than that of Ge/In<sub>2</sub>Se<sub>3</sub> (1.1 eV).

For both interfaces, the region of absorption is wide enough to nominate the interface for optoelectronic applications.

In order to obtain information about the energy band gap, the Tauc equation,  $(\alpha E)^n - E$  ( $\alpha = A/d$ ) for direct ( $n = 2$ ) and allowed electronic transitions are plotted and displayed in Fig. 3 (b). As the inset of the figure shows, the germanium substrate exhibited indirect ( $n = 1/2$ ) types of electronic transitions with an energy band gap of 0.60 eV. The coating of the Ge with Indium selenide reveal a direct allowed transitions energy band gap value of 1.60 eV. On the other hand, as clearly appears in Fig. 3 (b), the deposition of the  $\text{Ga}_2\text{S}_3$  films onto the  $\text{Ge}/\text{In}_2\text{Se}_3$  surface displayed two energy band gap values of 2.6 and 1.9 eV in the high ( $E > 3.3$  eV) and low ( $2.0 < E < 3.3$  eV) absorption regions, respectively. Since the formed Indium selenide on top of Ge refers to the  $\text{In}_2\text{Se}_3$  phase, the experimentally determined energy band gap for this phase when deposited onto glass substrates is 1.85 eV ( $\gamma - \text{In}_2\text{Se}_3$ ). The value is consistent with literature data [5, 9]. The lowering of the  $\text{In}_2\text{Se}_3$  energy band gap from 1.85 to 1.60 eV upon replacement of glass by germanium may be due to the band bending mechanism in addition to the electron-hole recombination mechanisms that occurred at the  $\text{Ge}/\text{In}_2\text{Se}_3$  interface. The electron affinity of  $p$ -type Ge is 4.13 eV [6] and that of  $n$ -type  $\gamma - \text{In}_2\text{Se}_3$  is 3.60 eV [10]. The 3.60 eV value is very different from those we previously reported for Indium selenide monophase as 4.55 eV [5] during the discussion of the Ge nanosandwiching between two layers of Indium selenide. In accordance with the published data [5, 6, 10] the conduction band offset ( $\Delta E_c = |q\chi_{\text{Ge}} - q\chi_{\text{In}_2\text{Se}_3}|$ ) at the  $\text{Ge}/\text{In}_2\text{Se}_3$  interface is 0.53 eV. With the energy band gaps differences being  $\Delta E_g = |E_{g-\text{Ge}} - E_{g-\text{In}_2\text{Se}_3}|$  1.25 eV, the conduction band offset ( $\Delta E_v = \Delta E_g - \Delta E_c$ ) turn out to be 0.72 eV. When the energy band gap that was determined from the  $E$ -axis crossings of Fig. 3 (b) is used, the values of  $\Delta E_g$ ,  $\Delta E_c$  and  $\Delta E_v$  are found to be 1.0, 0.53 and 0.47 eV, respectively. The valence and conduction band offsets support the assignment of the band bending as a reason for the shift in the energy band gap of  $\gamma - \text{In}_2\text{Se}_3$  when deposited onto Ge film instead of glass. On the other hand, at the  $\text{In}_2\text{Se}_3/\text{Ga}_2\text{S}_3$  interface, with the electron affinity and energy band gap of  $\text{Ga}_2\text{S}_3$  being 3.30 and 2.96 eV, respectively, the energy band gaps difference, the conduction and valence band offsets are expected to exhibit values of 1.11, 0.30 and 0.81 eV, respectively. However, using the experimentally determined energy band gap values ( $E_{g-\text{Ge}/\text{In}_2\text{Se}_3} = 1.60$  eV and  $E_{g-\text{In}_2\text{Se}_3/\text{Ga}_2\text{S}_3} = 2.60$  eV (as band gap of  $\text{Ga}_2\text{S}_3$  deposited onto  $\text{In}_2\text{Se}_3$  of band gap of 1.60 eV (lowered by interfacing effects)) which are determined from the  $E$ -axis crossings of Fig. 3 (b), the values of  $\Delta E_g$ ,  $\Delta E_c$  and  $\Delta E_v$  become 1.0 eV, 0.30 and 0.70 eV, respectively. Both of the interfaces  $\text{Ge}/\text{In}_2\text{Se}_3$  and  $\text{In}_2\text{Se}_3/\text{Ga}_2\text{S}_3$  exhibit a sufficiently large valence band offsets that nominate the  $\text{Ge}/\text{In}_2\text{Se}_3/\text{Ga}_2\text{S}_3$  system for use in optoelectronic technology. The value of the offset being 0.70 eV suits the devices which are famous in realizing quantum confinements that are necessary to separate the generated electron-hole pairs through photoexcitation effects. This effect usually enhances the photocurrent and external quantum efficiency as well [11, 12].

Fig. 4 (a) and (b) illustrate the real ( $\epsilon_r$ ) and imaginary parts ( $\epsilon_{im}$ ) of the dielectric constant spectra. The dielectric constants values are calculated with the help of the previously reported methods [6] using the data of Fig. 2. As can be seen from Fig. 4 (a), the real part of the dielectric constant for the Ge exhibit the highest values for all incident light with energy larger than 1.30 eV. The  $\epsilon_r$  values for Ge increases with decreasing incident photon energy. It exhibits two peaks at 1.75 and 1.30 eV. The appearance of the dielectric peak at 1.75 eV was previously observed for nanoparticles of germanium being embedded in the matrix of  $\text{Al}_2\text{O}_3$  [13]. This peak was assigned to the variation in average particle size in combination with the matrix induced effect. It was also observed in the photoluminescence spectra of diamonds synthesized in the Mg-Ge-C system. The peaks are assigned to the germanium but the origin of this peak was stated as unknown [14]. The peak which is observed at 1.30 eV is most probably assigned to the indirect transitions between the Si which exists in the substrate and the amorphous Ge films [15] (Fig. 1 (b)). For  $E < 2.10$  eV, the  $\epsilon_r$  spectra of the  $\text{Ge}/\text{In}_2\text{Se}_3$  show a continuously increasing trend of variation with decreasing incident photon energy, indicating a linear ( $\epsilon_r(E) = -33.96E + 70.09$ ) dependence of the dielectric constant on energy. The increase in the dielectric constant values

upon the Ge/In<sub>2</sub>Se<sub>3</sub> formation should be assigned to the electron-hole pairing in the depletion region of the pn interface. The increase in the values of  $\epsilon_r$  with decreasing  $E$  is probably assigned to the ability of the oscillating atoms to rotate with the incident electric field. As the frequency decreases, a relatively sufficient time of molecular rotations become available [16]. On the other hand, the dielectric spectra of the real part for the Ge/In<sub>2</sub>Se<sub>3</sub>/Ga<sub>2</sub>S<sub>3</sub> interfaces, show a decrease in the magnitude of the dielectric constant which may due to the availability of freer electrons [16] that is associated with the presence of  $n$  - type Ga<sub>2</sub>S<sub>3</sub>. In addition, the spectra contained two resonance peaks being centered at 3.43 and 2.07 eV. These two peaks appeared as a result of the participation of the Ga<sub>2</sub>S<sub>3</sub> into the structure of the heterojunction device. While the 3.43 eV energy value corresponds to the direct transitions in the energy band gap of the  $\alpha$  -phase of Ga<sub>2</sub>S<sub>3</sub> [17], the peak centered at 2.07 eV is probably assigned to the transition between the Ga and Se atoms at the In<sub>2</sub>Se<sub>3</sub>/Ga<sub>2</sub>S<sub>3</sub> interface. The latter assignment arise from the fact that the direct electronic transitions in GaSe between the  $\Gamma_{4v}^- - \Gamma_{3c}^+$  points of the first Brillouin zone which take place at 2.12 eV [17].

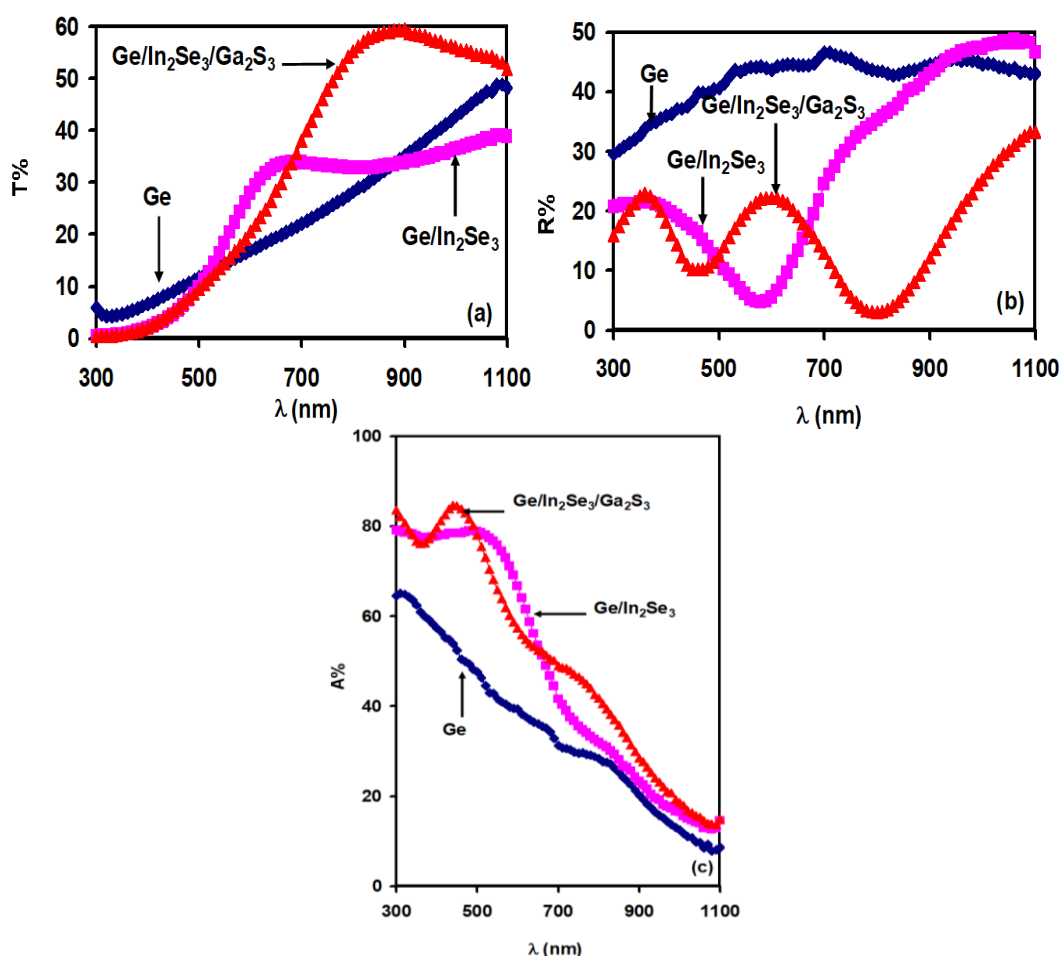


Fig. 2. (a) The transmission coefficient, (b) the reflection coefficient and (c) the absorbance spectra for the Ge, Ge/In<sub>2</sub>Se<sub>3</sub> and Ge/In<sub>2</sub>Se<sub>3</sub>/Ga<sub>2</sub>S<sub>3</sub> interfaces being recorded at room temperature.

The imaginary parts of the dielectric constant for the Ge, Ge/In<sub>2</sub>Se<sub>3</sub> and Ge/In<sub>2</sub>Se<sub>3</sub>/Ga<sub>2</sub>S<sub>3</sub> layers are shown in Fig. 4 (b). As the  $\epsilon_{im}$  value at particular frequency is directly proportion to the optical conductivity ( $\sigma(\omega) = \omega\epsilon_{im}/4\pi$ ), analyzing the imaginary part reveals information about the optical conduction parameters. The displayed  $\epsilon_{im}$  spectra indicate that the highest optical conduction refers to the Ge film. For Ge, the imaginary part increases with increasing incident photon energy reaching a maxima at 1.90 eV, then it decreases with increasing incident photon energy. Since the optical conductivity is directly proportional to the free charge carrier density ( $n$ )

and drift mobility ( $\mu$ ). The increasing trend of  $\varepsilon_{im}$  means freer charge carriers or higher drift mobility. The  $\varepsilon_{im}$  spectra for the Ge/In<sub>2</sub>Se<sub>3</sub> interface exhibit lower optical conductivity compared to that of Ge. This could have happened as a result of the formation of the depletion region between the *p*-Ge and *n*-In<sub>2</sub>Se<sub>3</sub>. The interface between two layers is usually associated with series resistance that decreases the conductivity. In addition to that the optical interference between the two layers lead to the appearance of the local (2.76 eV) and absolute maxima (1.46 eV) in the Ge/In<sub>2</sub>Se<sub>3</sub> heterojunction. For the same reasons, the optical spectra of the Ge/In<sub>2</sub>Se<sub>3</sub>/Ga<sub>2</sub>S<sub>3</sub> interface show lower values with two local (1.21 and 2.09 eV) and absolute maxima (3.27 eV).

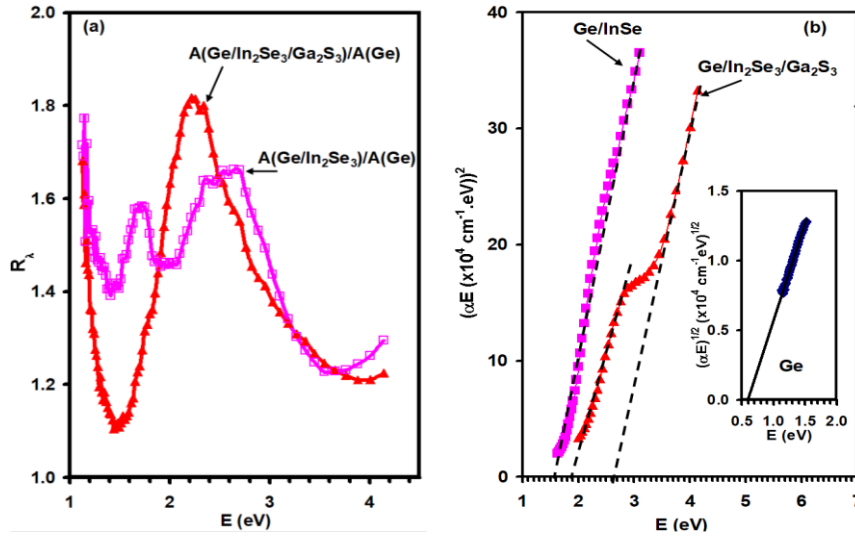


Fig. 3. (a) the absorbability spectra and (b) the Tauc equation plots for the Ge/In<sub>2</sub>Se<sub>3</sub>/Ga<sub>2</sub>S<sub>3</sub> interfaces.

The modeling of the imaginary part of the dielectric spectra in accordance with the Drude-Lorentz theory which was early described in our previous works [5, 6] using the equation,

$$\varepsilon_{im} = \sum_{i=1}^k \frac{w_{pe_i}^2 w}{\tau_i \left( (w_{e_i}^2 - w^2)^2 + w^2 \tau_i^{-2} \right)}, \quad (1)$$

with,  $\tau$ ,  $w_{pe} = \sqrt{4\pi n e^2 / m^*}$  and  $w_e$  being the free charge carrier relaxation time, the charge carrier bounded plasma frequency and the resonant frequency, It was possible to investigate the optical conduction parameters which are shown in Table 1. The effective mass ( $m^*$ ) values for Ge, In<sub>2</sub>Se<sub>3</sub> and Ga<sub>2</sub>S<sub>3</sub> were taken as  $0.374m_o$ , [6, 17]  $0.240m_o$  [6, 17] and  $0.40m_o$  [5, 17], respectively. The good consistency between the experimentally found data and theoretically estimated (dark solid plotting's in Fig. 4 (b)) are obtained assuming four linear oscillators that are subjected to electron frictional damping with coefficients of  $\tau_i^{-1}$ . In accordance with the tabulated data because the number of free charge carriers ( $n$ ) for each layer increase with increasing number of oscillators ( $i = 1 \dots k$ ), the most important oscillator is the first one. The amorphous layer of germanium exhibits the shortest relaxation time, the highest electron-plasmon resonant frequency, the highest free carrier density, the least drift mobility and the highest plasmon frequency. Interfacing the Ge with In<sub>2</sub>Se<sub>3</sub> decreased the free carrier density by ~nine times, increased the drift mobility from 5.02 to 18.5 cm<sup>2</sup>/Vs and shifts the plasmon frequency from 3.33 to 1.93 GHz. The main reason for these changes at the interface should be assigned to the formation of the depletion layer at the interface which leads to large amount of electron-hole recombination during the formation process in spite of the large valence band offsets as we

observed in this work. It is also possible to think that the large valence band offset which forces quantum confinement make the freedom of the charge carriers limited and as a result more space become available for the freely set electrons causing lesser collisions and thus making the scattering time longer. On the other hand, as Table 1 also shows, the coating of the Ge/ $\text{In}_2\text{Se}_3$  with  $\text{Ga}_2\text{S}_3$  significantly increased the scattering time, slightly decreased the resonant frequency ( $\omega_{e1}$ ) and decreased the free carrier density by additional 7.7 times compared to Ge/ $\text{In}_2\text{Se}_3$  and by 67.7 times compared to that of Ge. It also increased the drift mobility from 18.5 to 57.1  $\text{cm}^2/\text{Vs}$ . The plasmon frequency decreases to 0.77 GHz. We believe that the presence of the second valence band offset between the  $\text{In}_2\text{Se}_3/\text{Ga}_2\text{S}_3$  is the main reason for these remarkable enhancements in the optical conduction parameters. The quantum confinement at this interface reduces the free carriers more leading to a longer scattering times and better drift velocity of charge carriers in the response to the incident oscillatory electric field.

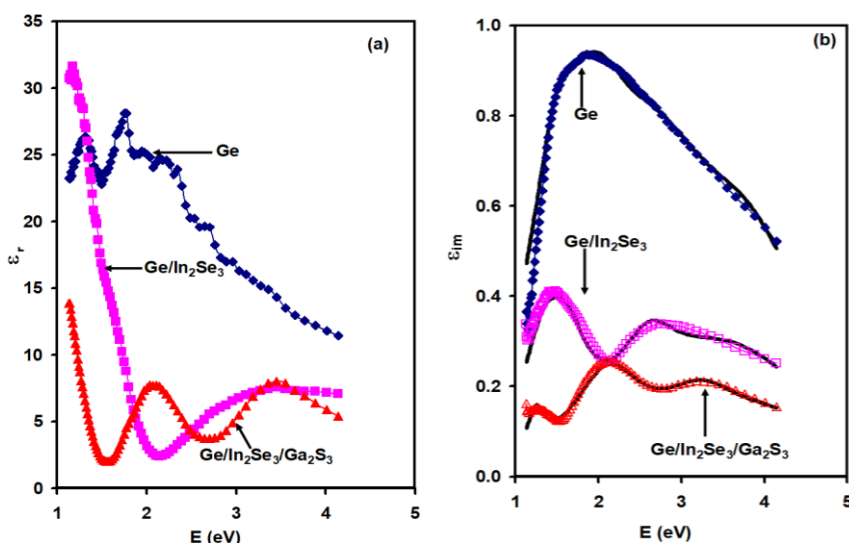


Fig. 4. (a) The real and (b) the imaginary parts of the dielectric spectra for the Ge, Ge/ $\text{In}_2\text{Se}_3$  and Ge/ $\text{In}_2\text{Se}_3/\text{Ga}_2\text{S}_3$  interfaces. The solid dark lines of (b) indicate the fittings obtained by Eqn. 1.

Compared to our previous works, the sandwiching of the  $\text{In}_2\text{Se}_3$  between Ge and  $\text{Ga}_2\text{S}_3$  improved the mobility from 15.6 to 57.1  $\text{cm}^2/\text{Vs}$  it also shifts the plasmon frequency from 2.30 to 0.77 GHz [5]. On the other hand, the sandwiching of the Ge between two Indium selenide layers was able to increase the drift mobility to 42.2  $\text{cm}^2/\text{Vs}$  [6]. The optimization of high drift mobility while maintaining the nanostructuring and quantum confinement effects are reported to be an asset in optoelectronic devices that guarantee smart operation modes [18] when employed in materials to reveal photodetectors, solar cells and thermoelectric devices. For our stacked layers (each of 200 nm thickness), the realizing of the high mobility and optimizing two quantum confinements at the two interfaces make the usability of the Ge/ $\text{In}_2\text{Se}_3/\text{Ga}_2\text{S}_3$  device favorable for carrying such issues.

Table 1. The computed optical conduction parameters for the Ge, Ge/In<sub>2</sub>Se<sub>3</sub> and Ge/In<sub>2</sub>Se<sub>3</sub>/Ga<sub>2</sub>S<sub>3</sub> heterojunctions.

	Ge				Ge/In <sub>2</sub> Se <sub>3</sub>				Ge/In <sub>2</sub> Se <sub>3</sub> /Ga <sub>2</sub> S <sub>3</sub>			
$\tau_i$ (fs)	0.80	0.63	0.35	0.32	1.00	1.00	0.75	0.24	2.5	0.60	0.50	0.37
$w_{ei}$ ( $\times 10^{15}$ rad/s)	2.35	3.10	4.30	6.00	2.08	2.50	4.00	5.80	1.90	3.30	5.00	6.50
$n$ ( $\times 10^{17}$ cm <sup>-3</sup> )	88.0	130	400	490	10.0	10.0	18.0	150.0	1.30	21.0	25.5	32.0
$\mu$ (cm <sup>2</sup> /Vs)	5.02	3.95	2.20	2.01	18.5	18.5	13.9	4.44	57.1	13.7	11.4	8.45
$w_{pei}$ (GHz)	3.33	4.05	7.10	7.86	1.93	1.93	2.59	7.47	0.77	3.10	3.42	3.83

#### 4. Conclusions

In this work we have shown the ability of forming a heterojunction with two valence and conduction band offsets that support the increase in the light absorbability through quantum confinement of charge carriers. The heterojunction which is formed from In<sub>2</sub>Se<sub>3</sub>/Ga<sub>2</sub>S<sub>3</sub> deposited onto Ge substrate exhibit energy band gap values that nominate it for electromagnetic waves sensing in the spectral range of ~1.0-3.0 eV. In addition, the interfacing of the Ge with In<sub>2</sub>Se<sub>3</sub> and with Ga<sub>2</sub>S<sub>3</sub> is found to be beneficial for the engineering of the dielectric properties and the optical conductivity parameters.

The modeling of the imaginary part of the dielectric constants spectra have shown that the drift mobility of the Ge/In<sub>2</sub>Se<sub>3</sub> can be remarkably increased via participation of the Ga<sub>2</sub>S<sub>3</sub> layers. The identified parameters presented by the plasmon frequency, free carrier density, scattering time and charge carrier resonant frequency values suggest the ability of using the Ge/In<sub>2</sub>Se<sub>3</sub>/Ga<sub>2</sub>S<sub>3</sub> heterojunctions as plasmonic devices with conduction parameters of the device being suitable for visible light communications in which our heterojunction can be employed as optical receivers.

#### Acknowledgments

The authors would like to acknowledge with thanking, the Deanship of Scientific Research (DSR) at the Arab American university for their support.

#### References

- [1] Kumar, Parveen, and Sanjeev Kumar Sharma, Silicon 13, no. 11 (2021): 4067-4074; <https://doi.org/10.1007/s12633-020-00718-5>
- [2] Srinivasan, Srinivasan Ashwyn, Joris Lambrecht, M. Berciano, Sebastien Lardenois, Philippe Absil, Johan Bauwelinck, Xin Yin, Marianna Pantouvaki, and Joris Van Campenhout. "Highly sensitive 56 Gbps NRZ O-band BiCMOS-silicon photonics receiver using a Ge/Si avalanche photodiode." In 2020 Optical Fiber Communications Conference and Exhibition (OFC), pp. 1-3. IEEE, 2020; <https://doi.org/10.1364/OFC.2020.W4G.7>
- [3] Aprojanz, Johannes, Ph Rosenzweig, TT Nhung Nguyen, Hrag Karakachian, Kathrin Küster, Ulrich Starke, Mindaugas Lukosius et al., ACS applied materials & interfaces 12, no. 38 (2020): 43065-43072; <https://doi.org/10.1021/acsami.0c10725>
- [4] AlGarni, Sabah E., and A. F. Qasrawi. Physica Scripta 95, no. 6 (2020): 065801; <https://doi.org/10.1088/1402-4896/ab7c78>

- [5] Al Garni, S. E., Olfat A. Omareye, and A. F. Qasrawi. *Optik* 144 (2017): 340-347; <https://doi.org/10.1016/j.ijleo.2017.06.109>
- [6] Al Garni, S. E., and A. F. Qasrawi. *Journal of Electronic Materials* 46, no. 8 (2017): 4848-4856; <https://doi.org/10.1007/s11664-017-5462-4>
- [7] Zhang, Han, Stéphane Virally, Qiaoliang Bao, Loh Kian Ping, Serge Massar, Nicolas Godbout, and Pascal Kockaert. *Optics letters* 37, no. 11 (2012): 1856-1858; <https://doi.org/10.1364/OL.37.001856>
- [8] Furbo, Simon, and L. Jivan Shah. *Solar Energy* 74, no. 6 (2003): 513-523; [https://doi.org/10.1016/S0038-092X\(03\)00186-5](https://doi.org/10.1016/S0038-092X(03)00186-5)
- [9] Wan, Tsz Lok, Jing Shang, Yuantong Gu, and Liangzhi Kou, *Advanced Materials Technologies* (2021): 2100463; <https://doi.org/10.1002/admt.202100463>
- [10] Chen, Shuo, Xuemei Liu, Xvsheng Qiao, Xia Wan, Khurram Shehzad, Xianghua Zhang, Yang Xu, and Xianping Fan, *Small* 13, no. 18 (2017): 1604033; <https://doi.org/10.1002/sml.201604033>
- [11] Diao, Senlin, Xiujuan Zhang, Zhibin Shao, Ke Ding, Jiansheng Jie, and Xiaohong Zhang, *Nano Energy* 31 (2017): 359-366; <https://doi.org/10.1016/j.nanoen.2016.11.051>
- [12] Jia, Lujian, Guopeng Fan, Wei Zi, Xiaodong Ren, Xiaojing Liu, Bin Liu, and Shengzhong Frank Liu, *Solar Energy* 144 (2017): 635-642; <https://doi.org/10.1016/j.solener.2017.01.042>
- [13] Das, Samaresh, Rakesh Aluguri, Santanu Manna, Rajkumar Singha, Achintya Dhar, Lorenzo Pavesi, and Samit Kumar Ray, *Nanoscale research letters* 7, no. 1 (2012): 1-11; <https://doi.org/10.1186/1556-276X-7-143>
- [14] Komarovskikh, Andrey, Alexey Dmitriev, Vladimir Nadolinny, and Yuri Palyanov, *Diamond and Related Materials* 76 (2017): 86-89; <https://doi.org/10.1016/j.diamond.2017.04.013>
- [15] Hart, John, Ramsey Hazbun, David Eldridge, Ryan Hickey, Nalin Fernando, Thomas Adam, Stefan Zollner, and James Kolodzey, *Thin Solid Films* 604 (2016): 23-27. <https://doi.org/10.1016/j.tsf.2016.03.010>
- [16] A. J. Moulson AJ, J. M. Herbert, *Electroceramics: materials, properties, applications*, John Wiley & Sons, 2003; <https://doi.org/10.1002/0470867965>
- [17] O. Madelung, *Semiconductors: data handbook*. Springer Science & Business Media, New York, 2012.
- [18] Evers, Wiel H., Juleon M. Schins, Michiel Aerts, Aditya Kulkarni, Pierre Capiod, Maxime Berthe, Bruno Grandidier et al., *Nature communications* 6, no. 1 (2015): 1-8; <https://doi.org/10.1038/ncomms9195>